Nonlinear transport at the strong intra-dot Coulomb interaction

2006 J. Phys.: Condens. Matter 18 L55

(http://iopscience.iop.org/0953-8984/18/5/L01)

INSTITUTE OF PHYSICS PUBLISHING JOURNAL OF PHYSICS: CONDENSED MATTER

J. Phys.: Condens. Matter **18** (2006) L55–L61 doi:10.1088/0953-8984/18/5/L01

LETTER TO THE EDITOR

Nonlinear transport at the strong intra-dot Coulomb interaction

I Sandalov[1] **and R G Nazmitdinov**[2,3,4]

[1] Department of Condensed Matter Physics, Royal Institute of Technology, Electrum 229, SE-164 40 Stockholm-Kista, Sweden
[2] Departament de Física, Universitat de les Illes Balears, E-07122 Palma de Mallorca, Spain
[3] Max-Planck-Institut für Physik komplexer Systeme, D-01187 Dresden, Germany
[4] Bogoliubov Laboratory of Theoretical Physics, Joint Institute for Nuclear Research, 141980 Dubna, Russia

E-mail: rashid@thsun1.jinr.ru

Received 20 December 2005
Published 20 January 2006
Online at stacks.iop.org/JPhysCM/18/L55

Abstract

Nonlinear transport is studied in the limit of weak and strong intra-dot Coulomb interaction. The nonequilibrium self-consistent mean-field equations for one-electron transition energies of an open dot and their spectral weights are derived at the strong Coulomb interaction. In this limit populations of states involved in tunnelling equalize upon the increase of the bias-voltage window even at low temperature. This results in a simple analytical relation between the heights of the current steps and the degeneracy of a spectrum in a two-dimensional parabolic dot in a magnetic field.

(Some figures in this article are in colour only in the electronic version)

Recently, in experiments with a small quantum dot (QD) in the Coulomb-blockade regime [1], a fine structure was observed in the conductance as a function of gate voltage versus source–drain voltage. It was suggested that this phenomenon is mainly due to co-tunnelling [2]. The theory of co-tunnelling [2], however, neglects specific quantum effects caused by a strong Coulomb interaction (SCI), which affect the transition energies and the tunnelling rates. On the other hand, numerous papers devoted to quantum effects in transport through QDs are focused on the analysis of the Kondo phenomenon in *single-level* QD models (cf [3]) in a linear-response regime, which is well understood nowadays. However, single-electron spectroscopy clearly indicates that the shell structure of small dots plays an essential role in the transport at low temperatures and weak dot–lead coupling [4]. This becomes more evident when the confining energy exceeds the charging energy [5] (hereafter, this regime is called a weak Coulomb interaction (WCI) regime). One of our goals is to present a self-consistent approach to nonlinear transport through a *multilevel* QD in the SCI regime. We will demonstrate that even in this

regime the shell structure of a small dot can be extracted from the analysis of nonlinear current as a function of a finite bias voltage. We will also show that the conductance inside the Coulomb diamond is governed by the spectral weights of one-electron transitions that complement the co-tunnelling picture.

We consider a QD coupled to the left and right leads with free electrons, described by the model Hamiltonian $H = H_l + H_r + H_{\rm QD} + H_t$. The term $H_\lambda = \sum_{k,\sigma} \varepsilon_{k\sigma} c^\dagger_{k\sigma} c_{k\sigma}$ describes noninteracting electrons with the energy $\varepsilon_{k\sigma}$, wavenumber k and spin σ in the lead $\lambda = l, r$. The closed dot is modelled by $H_{\rm QD} = \sum_p \varepsilon_p n_p + \sum_{p\neq p'} U_{pp'} n_p n_{p'}$ ($n_p = d^\dagger_p d_p$). Tunnelling between the dot and leads is described by the term $H_t = \sum_{p;k,\sigma\in l,r} v_{k\sigma;p} c^\dagger_{k\sigma} d_p$.

Suppose that the eigenvalue problem for the closed dot with interacting electrons is solved, i.e. $H_{\rm QD}|m\rangle = E_m|m\rangle$. Here m is a composite index for many-body states: $m = \{Q_m, N_m\}$, where Q_m is a set of quantum numbers of N_m-particle eigenstates; $N_m = 0, 1, \ldots, N$. Using the Hubbard operator $X^{mn} \equiv |m\rangle\langle n|$ that represents the transition from the state $|n\rangle$ to the state $|m\rangle$, the dot Hamiltonian can be written in a diagonal form $H_{\rm QD} = \sum_m E_m X^{mm}$ with the normalization condition $\{d_p, d^\dagger_p\} = \sum_m X^{mm} = 1$. For the tunnelling Hamiltonian we obtain $H_t = \sum_{n,m;k,\sigma\in l,r} v_{k\sigma;n,m} c^\dagger_{k\sigma} X^{nm}$, where $v_{k\sigma;n,m} = \sum_p v_{k\sigma;p}\langle n|d_p|m\rangle$. Below, we focus on transport in the resonant tunnelling regime, where Kondo physics is not involved.

Following [6], we obtain for the 'left/right' steady current:

$$J_{l(r)} = \frac{{\rm i}e}{\hbar}\int \frac{{\rm d}\omega}{2\pi} \sum_{bd} \Gamma^{l(r)}_{db}(\omega)\{G^<_{bd}(\omega) + f_{l(r)}(\omega)[G^R_{bd}(\omega) - G^A_{bd}(\omega)]\}. \qquad (1)$$

Equation (1) is derived in terms of Green functions (GFs) $G_{b\bar d}(t,t') = -{\rm i}\langle T X^b(t) X^{\bar d}(t)\rangle$ defined for the Hubbard operators. Hereafter, $a, b, c, \ldots$ denote Fermi-like transitions $X^a = |Q_m, N_m\rangle\langle Q'_n, N_n|$ and $X^{\bar a} = |Q'_n, N_n\rangle\langle Q_m, N_m|$ ($N_n = N_m + 1$) (as distinguished from Bose-like transitions, $X^\xi = |Q_m, N_m\rangle\langle Q'_m, N'_m|$ ($N'_m = N_m, N_m \pm 2$)). The commutation relations are $\{X^b, X^{\bar d}\} = \varepsilon^{b\bar d}_\xi X^\xi$, $[X^b, X^\xi] = \alpha^{b\xi}_c X^c$, where $\varepsilon^{b\bar d}_\xi$ and $\alpha^{b\xi}_c$ are the structure constants of the algebra and a summation over repeating indices is implied. The width function in equation (1) is $\Gamma^{l/r}_{db}(\omega) = \sum v^{l/r}_{d,k\sigma}\delta(\omega - \varepsilon^{l/r}_{k\sigma}) v^{l/r}_{k\sigma,b}$ and $f_{l/r}(\omega) = [1 + \exp\{\beta(\omega - \mu_{l/r})\}]^{-1}$, where $\mu_{l/r}$ is a chemical potential in the left/right lead and $\beta = 1/kT$. We consider the wide-band case. Then, the tunnelling matrix elements and the density of conduction electron states g_0 are slow functions of energy, i.e. $|v^{l/r}_{k\sigma,b}|^2 \simeq |\bar v_{l/r}|^2$ and $g^{l/r}_0(\omega) \simeq g^{l/r}_0$ and, therefore, $\Gamma^{l/r}_{db}(\omega) \simeq \Gamma^{l/r}_d = \pi \bar v^2_{l/r} g^{l/r}_0$. To shed light on the quantization effects in resonant transport, we consider a weak dot–lead coupling, using the coupling $\bar v_{l/r} g^{l/r}_0 \ll 1$ as a small parameter of the theory.

The GFs for a real time are calculated with the aid of GFs G_{bd} for an imaginary time, which are obtained by means of the diagram technique developed in [7] (below we refer to this as I). The basic idea therein is to introduce Schwinger–Kadanoff–Baym auxiliary sources ($T\exp\{{\rm i}\int U_\xi X^\xi\}$) for the Hubbard operators X^ξ. This allows us to construct a closed equation for the Hubbard GFs in terms of functional derivatives with respect to these sources, $D_0^{-1} G = P + V(P + {\rm i}\delta/\delta U)G$, where $P^{c\bar b} = \langle\{X^c, X^{\bar b}\}\rangle_U$. Iterations of this equation generate a perturbation expansion with respect to the interaction $V_{ab} = \sum_{\lambda,k\sigma\in\lambda} v^\lambda_{k\sigma,a} C^{(0)\lambda}_{k\sigma} v^\lambda_{k\sigma,b}$, where $C^{(0)}_{k\sigma} = -{\rm i}\langle T c_{k\sigma}(t) c^\dagger_{k\sigma}(t')\rangle$ is a bare GF of conduction electrons in the lead λ. The equation for zero GF is $D^{-1}_{0a} G^0_a = P^{a\bar a}_0$, where the inverse locator $D^{-1}_{0a} = {\rm i}\partial_t - \Delta_{\bar a}$, $\Delta_{\bar a} = E_{Q,N+1} - E_{Q',N}$ and $P^{a\bar a}_0 = \langle\{X^a, X^{\bar a}\}\rangle^{(0)}$. The perturbation V dresses both the locator D_{0a} and so-called end-factor $P^{a\bar a}_0$. Since the right-hand side of the exact equation for the GF contains P, GF is sought in the form $G_{a\bar b} = D_{ac} P^{c\bar b}$.

In this paper we use a mean-field approximation (MFA), where $D = D_0 + D_0(VP + \Sigma^{\rm loop})D$. Here $\Sigma^{\rm loop} = {\rm i}VD(\delta D_0^{-1}/\delta U)$ (see also equation (I.93)). The well-known Hubbard-I approximation (see equation (I.75)) is obtained from the MFA by neglecting $\Sigma^{\rm loop}$. The nondiagonal terms involve, obviously, higher orders of the small parameter and we neglect them.

Performing an analytical continuation of all the above equations from an imaginary time axis to the Keldysh contour, we obtain $G^{R/A}_{a\bar{a}} = (\omega - \Delta_{\bar{a}} \pm {\rm i}\Gamma_a P^{a\bar{a}})^{-1} P^{a\bar{a}}$ with $\Gamma_a = \Gamma^l_a + \Gamma^r_a$. The 'lesser' GF has the form $G^<_{a\bar{a}} = G^R_{a\bar{a}} V^<_{\bar{a}a} G^A_{a\bar{a}} = P^{a\bar{a}}\, \bar{f}_a L_a$. Here, $\bar{f}_a \equiv \alpha^l_a f_l + \alpha^r_a f_r$, $\alpha^{l/r}_a = \Gamma^{l/r}_a / \Gamma_a$. The Lorentzian $L_a = (P^{a\bar{a}}\Gamma_a/\pi)/[(\omega - \Delta_{\bar{a}})^2 + (P^{a\bar{a}}\Gamma_a)^2]^{-1}$ depends on two unknowns: $P^{a\bar{a}}$ and $\Delta_{\bar{a}}$. The quantities $P^{a\bar{a}}$ can be found via the 'lesser' Green function by making use of multiplication rules for the Hubbard operators at coinciding times, e.g. $\langle X^{mn}(t)X^{nm}(t)\rangle = \langle X^{mm}(t)\rangle = N_m(t)$. Since all GFs depend on the population numbers (via $P^{a\bar{a}}$), the relation $N_m = -{\rm i}\int {\rm d}\omega\, G^<_{a\bar{a}}(\omega)$ is, actually, the equation of self-consistency, which should be supplemented with the normalization condition $\sum_m N_m = 1$. All above equations are valid for a finite strength of the electron–electron interaction $U_{pp'}$.

Below, we consider a strong Coulomb interaction (SCI) limit, $U \to \infty$. In this limit the normalization condition becomes $X^{00} + \sum_p X^{pp} = 1$, $P^{a\bar{a}} \to P_{0p} = \langle X^{pp}\rangle + \langle X^{00}\rangle \equiv N_0 + N_p$, while $H_{\rm QD} \to \tilde{H}_{\rm QD} = E_0 X^{00} + \sum_p \varepsilon_p X^{pp}$ and $H_t \to \tilde{H}_t = \sum_{p;k,\sigma\in l,r} v_{k\sigma;p} c^\dagger_{k\sigma} X^{0p}$. Note that at zero coupling to the leads one-electron energies coincide in both WCI and SCI regimes. This fact opens a nice opportunity to study in a transparent way the role of the Coulomb interaction within this particular charge sector.

Let us choose $E_0 = 0$ and assume that the electrochemical potentials of the metals are placed within the region of the lowest transitions $[0, p]$, i.e. at zero bias voltage $\mu_l = \mu_r \sim \Delta^{(0)}_{p0} \equiv (\varepsilon_p - E_0) = \varepsilon_p$. Calculating GFs according to the procedure described above, we obtain from equation (1) in the limit $U \to \infty$:

$$J = \frac{2e}{\hbar}\int {\rm d}\omega \sum_p P_{0p} L_p(\omega) \bar{\Gamma}_p \left[f_l(\omega) - f_r(\omega)\right], \tag{2}$$

where $\bar{\Gamma}_p = \Gamma^l_p \Gamma^r_p / \Gamma_p$ and

$$N_p = -{\rm i}\int {\rm d}\omega G^<_{0p,p0}(\omega) = P_{0p}\int {\rm d}\omega L_p(\omega)\bar{f}_p(\omega), \qquad N_0 + \sum_p N_p = 1. \tag{3}$$

The coupling to the contacts renormalizes bare transition energies $\Delta^{(0)}_{p0} = \varepsilon_p$; namely, $\Delta_{p0} = \Delta^{(0)}_{p0} + \Sigma^{\rm loop}$, or, explicitly,

$$\Delta_{p0} \simeq \varepsilon_p + 4\int {\rm d}\omega \sum_{p_1 \neq p} (\omega - \Delta_{p_1 0}) L_{p_1}(\omega)\bar{f}_{p_1}(\omega)/P_{0p_1}. \tag{4}$$

The expression for the current, equation (2), and the system of equations (3), (4) for a multilevel dot, obtained within a nonequilibrium mean field theory, are our central result. Equation (4) does not contain self-interaction: the renormalization occurs due to admixture of all *other* transitions (excluding the nonelastic co-tunnelling [2]). We recall that a master-equation approach (cf [8]) does not provide the widths in Lorentzians, the level shifts, equation (4), and misses the self-consistency in the population of states. The shifts are absent in the Hubbard-I approximation as well. Note that for the WCI regime the current is determined by the same equation (2), where one should put $P_{0p} = 1$ and $\Delta_{p0} = \varepsilon_p$.

At $\Gamma \ll kT < \Delta_{p0}$ ($\beta\Gamma \ll 1$) the integrals can be calculated analytically. For symmetric coupling ($\Gamma^l_p = \Gamma^r_p = \Gamma_p/2$) we have for the current

$$J = \frac{e}{2\hbar}\sum_p \Gamma_p P_{0p}\left[f_l(\Delta_{p0}) - f_r(\Delta_{p0})\right]. \tag{5}$$

The analogy with the Landauer–Büttiker formula is obvious: the current is still proportional to the number of channels involved. The difference is that in the SCI regime each channel contributes with its own spectral weight P_{0p} and both the energies Δ_{p0} and the spectral weights P_{0p} of the transitions must be found self-consistently. These effects are specific for the transport in the SCI regime and are missing in the theory of co-tunnelling [2].

At $\beta\Gamma \ll 1$, in the first order of the coupling parameter, the equations for population numbers, equations (3), are solved analytically:

$$N_0 = \left(1 + \sum_p \Phi_p\right)^{-1}, \qquad N_p = \Phi_p \left(1 + \sum_p \Phi_p\right)^{-1},$$
$$\Phi_p = \mathrm{e}^{-\beta(\Delta_{p0}-\mu)} \frac{\mathrm{e}^{-\beta(\Delta_{p0}-\mu)} + \cosh(\beta eV/2)}{1 + \mathrm{e}^{-\beta(\Delta_{p0}-\mu)} \cosh(\beta eV/2)}. \tag{6}$$

Here $\mu \equiv (\mu_l + \mu_r)/2$. At $eV \to 0$ the Gibbs' statistics for in-dot states are restored at the Fermi energy of metals. At low temperature $kT < \Delta_{p0}$ and fixed $\mu < \Delta_{p0}$, when $2(\Delta_{p0} - \mu) < eV \ll U$, for the states located in the 'conductive window' $\mu_r < \Delta_{p0} < \mu_l$ (CW) the magnitude $\Phi_p \to 1$ and $N_0 = N_p = 1/(n_W + 1)$. Here, n_W is the number of one-electron states involved into the resonant tunnelling. Thus, *the applied bias voltage equalizes the population numbers of the states within the CW at the SCI regime. Moreover, the lower the temperature the faster this process sets in*.

Now, we focus on shell effects that are much stronger than spin effects and have as yet not been discussed in literature relating to quantum transport. We recall that for the closed dot one-electron states are the same for the WCI and SCI regimes. Let us consider a dot with a circular shape, $\omega_x = \omega_y = \omega_0$ in a perpendicular magnetic field B (cf [9]). The dot eigenmodes are $\Omega_\pm = (\Omega \pm \omega_c/2)$ with $\Omega = \sqrt{\omega_0^2 + \omega_c^2/4}$ [10]. Here $\omega_c = \frac{|e|}{m^* c} B$.

At small eV and chosen fixed μ (or the gate voltage) the first transition $\Delta_{10} < \mu_r$ and the current, equation (5), is zero, in spite of $P_{0p} \neq 0$ ($N_0 = 1$) (see figure 1). At higher voltages the CW contains n_W electron states and, according to equations (3), (6), $P_{0p} = 2/(n_W + 1)$. As a result, the SCI current is $J_{\mathrm{SCI}} = 2J_0 n_W/(n_W + 1)$, where $J_0 = e\sum_p \Gamma_p/[2\hbar n_W] \equiv e\tilde{\Gamma}/(2\hbar)$. The WCI current, however, is $J_{\mathrm{WCI}} = J_0 n_W$. Thus, even for a large bias voltage eV, the SCI current is weaker than the WCI one, by factor of $\eta = J_{\mathrm{SCI}}/J_{\mathrm{WCI}} = 2/(n_W + 1)$ (until the other charge sector is not switched on at $eV \sim U$).

The effect of degeneracy of the spectrum becomes transparent at the specific values of the magnetic field

$$t_0 \equiv \omega_c/\omega_0 = (r - 1)/\sqrt{r} \tag{7}$$

where the ratio $r = \Omega_+/\Omega_- = 1, 2, 3, \ldots$. We consider first $r = 1$, i.e. zero magnetic field (figure 1). In this case, each shell k has the degeneracy $g_k = k + 1$. If in the transport window the last shell n is filled, the total number of states involved in the transport is $n_W + 1 = 2\sum_{k=0}^{n}(k+1) + 1 = n^2 + 3n + 3$ (the 2 is due to the spin degeneracy). Consequently, the height of the nth step in the SCI current is $J_{\mathrm{SCI}}/J_0 = 2(n+1)(n+2)/(n^2 + 3n + 3)$, which is smaller than the WCI current by factor $\eta = 2/(n^2 + 3n + 3)$. Since $\Phi_p \simeq \mathrm{e}^{-\beta(\Delta_{p0}-\mu)}[1 + \alpha\,(eV)^2]$ at small eV (see equations (6)), these effects cannot be seen in the linear conductance. Another effect (which is not seen in the master-equation approach) follows from equation (4): the coupling pushes the transition energies Δ_{p0} down compared with the bare energies ε_p, which decreases the bias voltage threshold for the current to be observed.

For $r = 2$ ($\omega_c/\omega_0 \simeq 0.7$) we find a new shell structure *as if* the confining potential were a deformed harmonic oscillator without a magnetic field. The number of levels are just the number of levels obtained from the two-dimensional oscillator with $\omega_> = 2\omega_<$ ($\omega_>$ and $\omega_<$

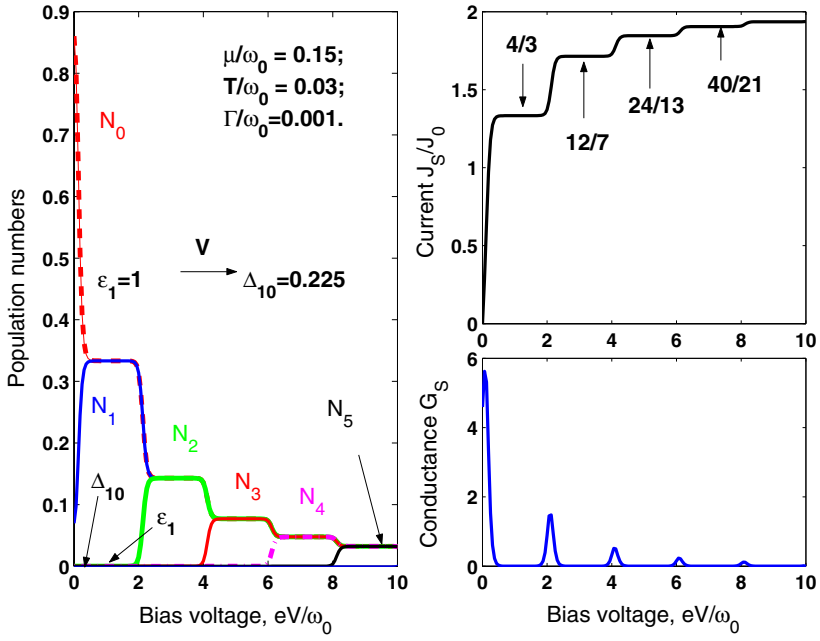

Figure 1. Population numbers N_p (left panel), the current J_S/J_0 and the conductance $G_S = \mathrm{d}J_S/\mathrm{d}(eV)$ as a function of the bias voltage (right panel) in the SCI regime at zero magnetic field. In each shell k we have $2(k+1)$ degenerate orbitals characterized by the same N_p ($p = k+1$). In particular, $N_0 = \langle X^{00}\rangle$, $N_1 = N_{k=0,\gamma_0=1} = N_{k=0,\gamma_0=2}$ etc, where γ_k is the orbital index in the shell k. Arrows at the bias voltage axis indicate the position of the bare ε_1 and the renormalized Δ_{10} energies from the shell $k = 0$. Their exact values and the parameters of the calculations are displayed in the left panel. In the right panel, the rational numbers characterize the height of the nth step in the SCI current, $J_{\mathrm{SCI}}/J_0 = 2(n+1)(n+2)/(n^2+3n+3)$, for the last filled shell n.

denote the larger and smaller value of the two frequencies). In this case $n_W = (n+2)^2/2$ if the last filled shell is even, and $n_W = (n+1)(n+3)/2$ if it is odd, and these numbers define the heights of steps in both the WCI (right panel of figure 2) and SCI regimes.

These features of the spectrum can be imaged by the conductance measurements. In particular, the results for the differential conductance $\mathrm{d}J/\mathrm{d}(eV)$ at the WCI regime (left panel of figure 3) resemble very much the experimental conductance discussed in [5]. An increase in the magnetic field brings in the CW states with a large magnetic quantum number $m = n_- - n_+$ and pushes up the ones with $-m$. This gives oscillations in the current. They are suppressed together with the current itself in the SCI regime. The shrinking of the parameter region with a non-zero current in the SCI regime is clearly seen from a comparison of the left and right panels of figure 3 plotted within the same scale. The amplified fine structure of the SCI conductance is displayed in the insertion. Although the shell structure is manifested in the fine structure in the SCI case too, it is strongly suppressed by the intra-dot correlations.

In summary, we derived the expression for the current, equation (2), through a multilevel dot at non-zero temperature in the nonequilibrium mean-field theory for the SCI regime. The nonlinear transport is determined by the spectral weights, equations (3), of the dot states, equation (4), renormalized due to the coupling to the leads. At strong Coulomb interaction and small coupling to the leads, the population numbers, calculated analytically, display an equalization at high bias voltages. In this limit we obtain a simple expression which relates the height of the nth step in the current to a number of states participating in the transport. In the

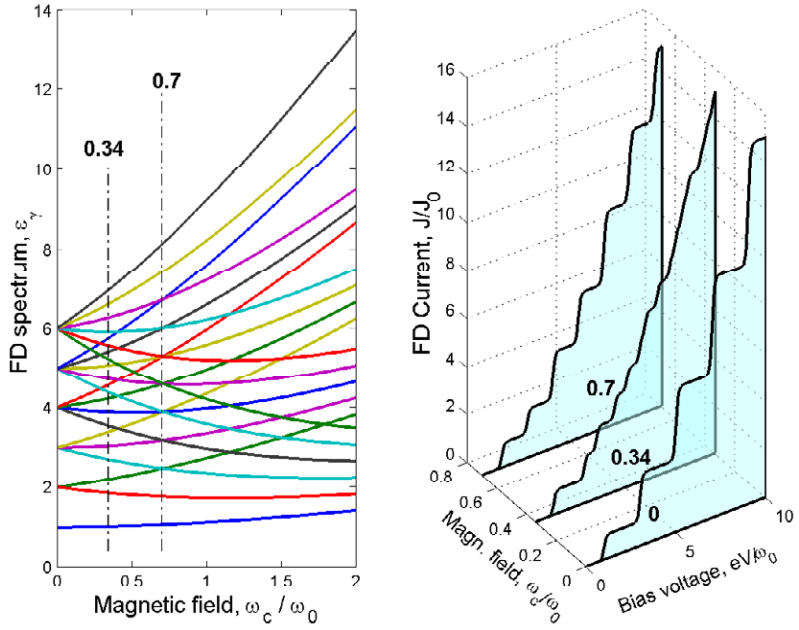

Figure 2. Magnetic field (ω_c/ω_0) dependence of: (a) the Fock–Darwin spectrum (in units ω_0); (b) the tunnelling current J_{WCI} (in units $J_0 = \bar{\Gamma}/4h$) through the quantum dot; arrows indicate the cuts in the planes that correspond to the fields $\omega_c/\omega_0 = 0.0, 0.34, 0.7$, respectively. The degeneracy at $\omega_c/\omega_0 = 0.0, 0.7$ is clearly seen in jumps of the current.

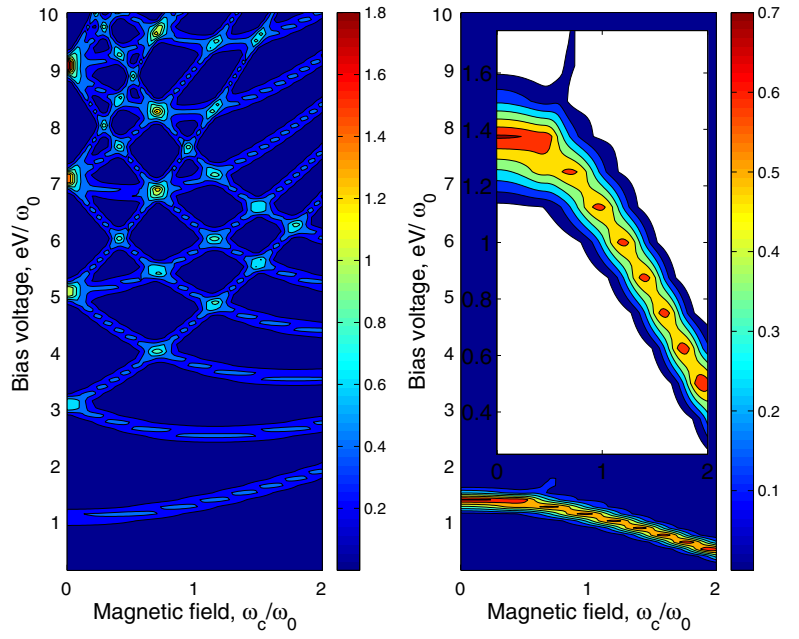

Figure 3. The magnetoconductance $G = \mathrm{d}J/eV$ at the WCI (left) and the SCI regimes (right). The WCI magnetoconductance displays the Fock–Darwin spectrum with clearly expressed shell structure. The SCI magnetoconductance is compressed due to the sum rule for population numbers and is very low above $2eV/\omega_0$. The insertion displays the structure of G in the region 0–1.8.

WCI regime, at specific values of the magnetic field, equation (7), we predict a drastic increase of the current through the dot due to the shell effects. Tuning the magnetic field near such specific points can be used to construct magnetic-field sensitive switch on–off devices.

This work was partly supported by grants PRIB-2004-9765 (Govern de les Illes Balears), BFM2002-03241 (MEC). IS is thankful to UIB for a financial support and RGN is grateful to the Ramón y Cajal programme (Spain).

References

[1] De Franceschi S *et al* 2001 *Phys. Rev. Lett.* **86** 878
Schleser R *et al* 2005 *Phys. Rev. Lett.* **94** 206805
[2] Averin D V and Nazarov Yu V 1990 *Phys. Rev. Lett.* **65** 2446–9
[3] Hershfield S *et al* 1991 *Phys. Rev. Lett.* **67** 3720–23
Aguado R and Langreth D C 2000 *Phys. Rev. Lett.* **85** 1946–9
Bulka B R and Lipinski S 2003 *Phys. Rev.* B **67** 024404
Lopez R and Sanchez D 2003 *Phys. Rev. Lett.* **90** 116602
Paaske J, Rosch A and Wolfle P 2004 *Phys. Rev.* B **69** 155330
[4] Kouwenhoven L P, Austing D G and Tarucha T 2001 *Rep. Prog. Phys.* **64** 701–36
[5] Ono K *et al* 2002 *Physica* B **314** 450–4
Ota T *et al* 2004 *Phys. Rev. Lett.* **93** 066801
[6] Jauho A P, Wingreen N S and Meir Y 1994 *Phys. Rev.* B **50** 5528–44
[7] Sandalov I, Johansson B and Eriksson O 2003 *Int. J. Quantum Chem.* **94** 113–43
[8] Golovach V N and Loss D 2004 *Phys. Rev.* B **69** 245327
[9] Heiss W D and Nazmitdinov R G 1998 *Pis. Zh. Eksp. Teor. Fiz.* **68** 870–5
Heiss W D and Nazmitdinov R G 1998 *JETP Lett.* **68** 915–21 (Engl. Transl.)
[10] Fock V 1928 *Z. Phys.* **47** 446
Darwin C G 1930 *Proc. Camb. Phil. Soc.* **27** 86